ELSEVIER

Neurocomputing 32–33 (2000) 173–180

NEUROCOMPUTING

www.elsevier.com/locate/neucom

Simulation techniques for localising and identifying the kinetics of calcium channels in dendritic neurones

Kelvin E. Jones*, Kevin P. Carlin, Jeremy Rempel, Larry M. Jordan, Robert M. Brownstone

Spinal Cord Research Centre, Department of Physiology, University of Manitoba, 730 William Ave., BMCB 406, Winnipeg, Manitoba, Canada R3E 3J7

Accepted 13 January 2000

Abstract

The present simulations were designed to determine whether the current–voltage (I–V) relationship obtained during voltage clamp was sufficient to characterise the kinetics and distribution of dendritic Ca^{2+} channels in spinal motoneurones. Two models were constructed, one based on a fully reconstructed adult cat motoneurone (neuromorphic model) the second a reduced two-compartment motoneurone model. The current–voltage (I–V) relationship in the neuromorphic model was used as a template to evaluate the I–V behaviour of the reduced model while simulating changes in location and kinetics of the calcium channels. The results show that the discriminative quality of the reduced model is low and the neuromorphic model remains the better qualitative match to the eletrophysiological results.

Keywords: Motoneurone; Plateau potential; Bistability; Calcium channel

1. Introduction

We recently presented evidence for dendritically located L-type calcium channels in "mature" spinal motoneurones of the mouse [3]. This evidence consisted of three parts: (1) immunohistochemical labelling of the alpha-1D subunit of neuronal calcium channels in dendritic membrane; (2) electrophysiological evidence for calcium

* Corresponding author. Tel.: + 1-204-789-3305; fax: + 1-204-789-3930.
E-mail address: kelvin@scrc.umanitoba.ca (K.E. Jones).

0925-2312/00/$ - see front matter
PII: S0925-2312(00)00160-0

currents outside of the region of space clamp; and (3) compartmental modelling that confirmed speculations based on the electrophysiology. The presence of a clockwise hysteresis in the current–voltage (I–V) curve during slow triangular voltage clamp protocols, is of particular interest in the current results. During the ascending phase of the voltage clamp an inward current was activated at a mean voltage of -46 mV (V_{on}). During the descending phase of the voltage clamp this persistent current did not deactivate until -83 mV (V_{off}). The I–V curve between these two voltages, V_{off} and V_{on}, showed two stable current levels for a given voltage. This type of I–V curve is a characteristic of bistability and closely resembles the stable theoretical solutions for the steady-state I–V curve [2].

Our previous results suggested that the neuromorphic model, based on a fully reconstructed adult cat motoneurone, produced a qualitatively similar I–V during triangular voltage-clamp protocols compared to the experimental results. That is, the V_{on} and V_{off} set the borders of a range of bistability. We then asked the question: *How do the location and activation properties of the calcium channels affect the values of* V_{on} *and* V_{off}? In an attempt to answer this question, we used a reduced two-compartment motoneurone model that would allow a greater exploration of parameter space while minimising computational overhead.

2. Methods

The morphology of a fully reconstructed adult cat motoneurone (courtesy of RE Burke) was incorporated into the NEURON simulation environment [8]. This neuromorphic model comprised 1484 compartments and was based on the HRP-stained motoneurone 43/5 reported previously [5,6]. Each compartment of the model had a specific membrane capacitance, $C_m = 1\ \mu F/cm^2$, axial resistance, $R_a = 70\ \Omega/cm$ and an equilibrium potential for the passive leak conductance, $E_{pas} = -65$ mV. The passive leak conductance, g_{pas}, was 9.1×10^{-5} S/cm^2 throughout the cell except in the soma where it was 4.4×10^{-3} S/cm^2 due to the non-specific shunt caused by impalement with the sharp intracellular electrode (see [6]).

The two-compartment minimal model was developed from Booth et al. [2]. The electrotonic-like parameters for this model included a coupling conductance, g_c, through which current flows between the soma and dendritic compartments, and ρ the somatic to total cell surface area ratio. The initial values were $g_c = 0.1$ mS/cm^2 and $\rho = 0.1$. The voltage of the dendritic compartment was represented by the following equation:

$$-C_m \frac{dV_D}{dt} = g_{leak}(V_D - 60) - \frac{g_c}{(1-\rho)}(V_S - V_D) + g_{Ca-L} m_L (V_D - E_{Ca}),$$

where $C_m = 1\ \mu F/cm^2$, V_D is the dendritic voltage (mV), the leak conductance $g_{leak} = 0.51$ mS/cm^2, the maximum calcium conductance density $g_{Ca-L} = 0.6$ mS/cm^2, m_L is the activation function for the calcium channels described below and $E_{Ca} = 60$ mV is the equilibrium potential for calcium. The somatic voltage, V_S, was controlled by

a slow triangular voltage command protocol as described in the results. The two-compartment model was very sensitive to the rate at which the voltage clamp was performed. A total duration of 2 min was used, as there was little change in the I–V with longer durations.

The only active conductance used in the models was a persistent L-type Ca^{2+} conductance that was located in the dendrites. In the neuromorphic model the conductance was located on dendrites third-order and greater based on the previously reported immunohistochemical data [3]. Calcium current in both the neuromorphic and minimal models was modelled with a steady-state activation function given by a Boltzmann equation:

$$m_{L\infty}(V) = \frac{1}{1 + \exp[(V - V_{1/2})/k]},$$

in which $V_{1/2}$ is the half-activation voltage and k is the slope factor. The voltage parameters of the L-type Ca^{2+} channels in the neuromorphic model were taken from the description of low-voltage-activated (LVA) L-type Ca^{2+} channels reported by Avery and Johnston [1], i.e. $V_{1/2} = -30$ mV and $k = 6$ mV. These parameters gave a good qualitative match to the previously reported electorphysiological results [3]. At each time step, the differential equation:

$$\frac{dm_L}{dt} = \frac{m_{L\infty}(V) - m_L}{\tau},$$

was solved where $\tau = 40$ ms is the time constant for activation. The maximal calcium conductance density was set in the two models to reproduce the peak current density measurements from the in vitro electrophysiological results in 2 mM Ca^{2+}, i.e. ~ 16 pA/pF [3]. The simulations of the reduced model were implemented in XPP written by G. Bard Ermentrout.

3. Results

A triangular voltage clamp protocol was applied to the soma compartment of the neuromorphic model in which the soma voltage ramped from -120 to 60 mV and back with a total duration of 2 min (Fig. 1A). The current needed to perform the voltage clamp is illustrated in the top panel of Fig. 1A. During the ascending ramp the dendritcally located L-type Ca^{2+} channels were activated producing an inward current with an onset voltage (V_{on}) of -47.5 mV. During the subsequent descending voltage ramp (Fig. 1A, grey line) the Ca^{2+} channels remained activated to voltage levels hyperpolarised with respect to V_{on}. Deactivation of the channels began at -65 mV, at the peak of the current, and continued until the somatic voltage command was -93 mV, V_{off} -65 to -93 mV (Fig. 1B). The difference between V_{on} and V_{off} and the resulting clockwise hysteresis in the I–V relationship is due to the dendritic location of the Ca^{2+} channels [3]. The LVA L-type Ca^{2+} channel description used in these simulations gave a good qualitative fit to the experimental

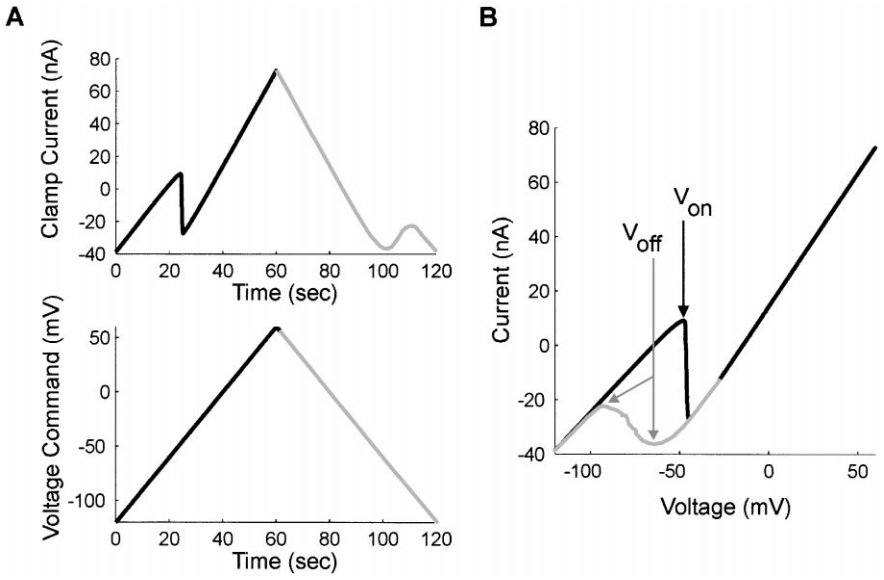

Fig. 1. The I–V curve of the neuromorphic model with dendritic LVA Ca^{2+} channels. A, voltage command applied to soma compartment (bottom) and the current measured during voltage-clamp protocol. B, I–V curve from the voltage-clamp protocol illustrated in panel A. During the ascending phase of the voltage-clamp protocol (black line) an inward current is activated at -47.5 mV, V_{on}. The current is persistent and remains activated during the descending phase of the voltage clamp protocol (grey line). Deactivation of the current begins at -65 mV and the current is fully deactivated by -93 mV, V_{off}. These values of V_{on} and V_{off} are generated when Ca^{2+} channels ($V_{1/2} = -30$ mV, $k = 6$ mV) are distributed on the dendrites and will serve as the template against which the I–V curves of the reduced model will be compared.

data [3]. However, other combinations of channel distribution and voltage parameters may have given an equally similar qualitative match to the electrophysiological results.

To explore the relationship between the I–V curves, the kinetics of Ca^{2+} channels and their distance from the soma, a reduced two-compartment model was constructed (Fig. 2A). The distance of the channels from the soma was simulated by changes in the coupling conductance, g_c, with larger values representing a close proximity to the soma and small values a relatively distant location electrotonically. A triangular voltage-clamp protocol was applied to the reduced model in which the soma compartment was ramped over a voltage range of 180 mV and back with a total duration of 2 min (i.e. with the same slope as the voltage command protocol used in the neuromorphic model). The long duration was needed to generate I–V curves that approached the steady state values.

The electrotonic distance of the channels from the soma modified the I–V curves. This effect is illustrated in Fig. 2B for two different values of g_c. With a relatively distant location, $g_c = 0.1$, there is a clear clockwise hysteresis in the I–V curve. When

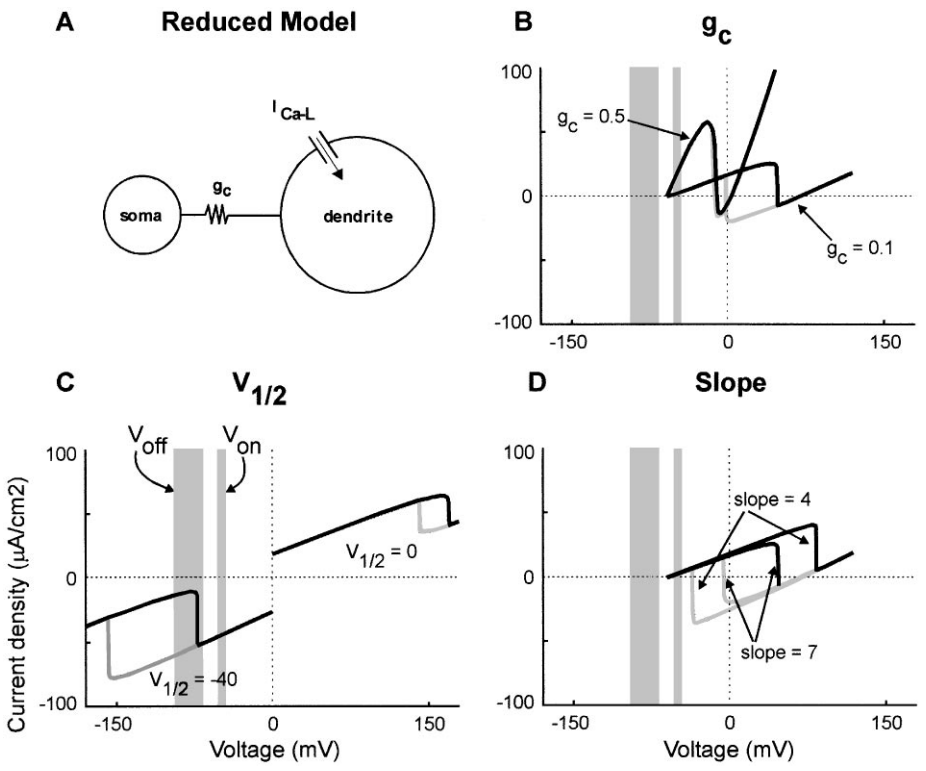

Fig. 2. I–V curves of the reduced model with variations in channel kinetics and location. A, the reduced two compartment model with Ca^{2+} channels in the dendrite separated from the soma by the coupling conductance, g_c. B, changes in relative electrotonic location of the Ca^{2+} channels are simulated by changes in g_c while $V_{1/2} = -20$ mV and $k = 7$ mV are held constant. At a relatively close location, $g_c = 0.5$, the I–V curves from the ascending and descending phase overlap. With an increased separation of the channels from the soma, $g_c = 0.1$, a hysteresis develops in the I–V curve. The value of V_{on} becomes more depolarised the smaller the value of g_c. C, effect of changes in $V_{1/2}$ on the I–V curve while $k = 7$ mV and $g_c = 0.1$ mS/cm^2 are held constant. The higher the voltage activation level of the channels the more depolarised the values of V_{on} and V_{off}. The shaded bars (reproduced in panels B and D) illustrate the target values of Von and Voff from the neuromorphic model. D, effect of changes in activation slope while $V_{1/2} = -20$ mV and $g_c = 0.1$ mS/cm^2 are held constant. The steeper the activation slope, the greater the difference between V_{on} and V_{off}.

the two compartments are more tightly coupled by setting $g_c = 0.5$, the hysteresis is abolished and V_{on} is shifted in the hyperpolarising direction. The effect of changes in the Ca^{2+} channel activation parameters on the I–V curves are illustrated in Fig. 2C and D. In Fig. 2C the effect of changing the half-activation voltage ($V_{1/2}$), while maintaining a constant activation slope (k) and g_c, are illustrated. With a $V_{1/2} = -40$ mV [2] the I–V curve showed a clockwise hysteresis with a $V_{on} = -79$ mV and a $V_{off} = -154$ mV. By shifting the $V_{1/2}$ to a typical HVA value

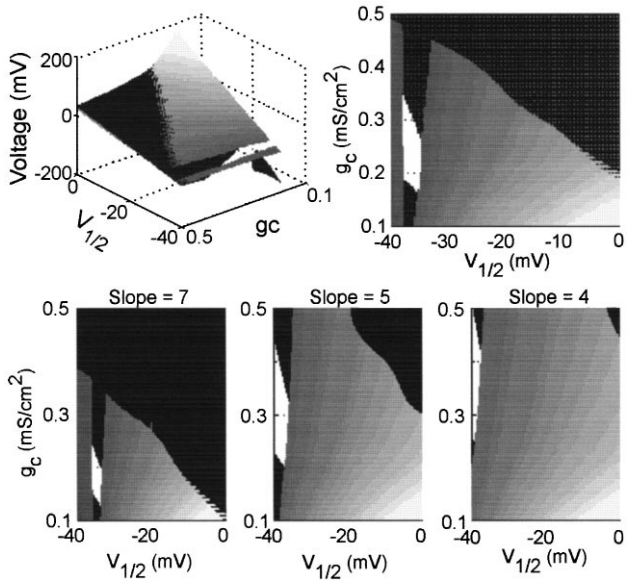

Fig. 3. Values of V_{on} and V_{off} in the reduced model over the parameter space tested. The top panel shows the values of V_{on} (grey surface) and V_{off} (black surface) for different combinations of $V_{1/2}$ and g_c while maintaining an activation slope of 6 mV (the same slope as that used in the neuromorphic model). At the border between the two surfaces $V_{on} = V_{off}$, but elsewhere the values diverge. The target values of V_{on} and V_{off}, determined from the neuromorphic model and illustrated by the shaded bars in Fig. 2, have been "cut out" of the respective surface leaving a hole in the surface that identifies the target values. Where the holes overlap in the two surfaces, white area in top right and bottom panels, are regions of parameter space where the I–V of the reduced model matches the target values. The reduced model fails to identify the channels in the neuromorphic model as uniquely $V_{1/2} = -30$ mV and slope = 6 mV. Instead there are wide areas of parameter space that give appropriate values of V_{on} and V_{off}.

of 0 mV [7] the I–V curve was shifted so that $V_{on} = 162$ mV and $V_{off} = 157$ mV. Therefore, a depolarising shift of $V_{1/2}$ resulted in unequal depolarising shifts of V_{on} and V_{off}. In like manner, changes in activation slope produced shifts in the V_{on} and V_{off} values of the I–V curves. This effect on the I–V is shown in Fig. 2D for a slope of 7 and 4 mV. With a steeper slope of 4 mV (typical of HVA Ca^{2+} channels, [7]) the V_{on} shifted in the depolarising direction while V_{off} shifted in the hyperpolarising direction.

In each of the I–V panels of Fig. 2 the areas representing the values of V_{on} and V_{off} in the neuromorphic model are shown by the shaded bars. The values of $V_{1/2}$, slope and g_c were then varied through a wide range of parameter space to determine whether a unique combination of parameters would situate the I–V of the reduced model within the areas of V_{on} and V_{off} from the neuromorphic model. The results of these simulations are illustrated in Fig. 3. In the top left panel of Fig. 3 the solutions for V_{on} (grey surface) and V_{off} (black surface) are shown for different combinations of $V_{1/2}$ and g_c using an activation slope of 6 mV. This value for the activation slope is the

one reported by Avery and Johnston [1] and used in simulations with the neuromorphic model. The values corresponding to the V_{on} and V_{off} areas in Fig. 2 have been "clipped" out of the surfaces leaving only area that does not correspond to the target values. The top right panel shows a top-down view of the same data. From this perspective, areas in parameter space that match both V_{on} and V_{off} appear as white space. The panel shows that with a $V_{1/2}$ between -35 to -38 mV and an activation slope of 6 mV the coupling conductance can range from 0.16 to 0.35 and generate an I–V curve that matches the results from the neuromorphic model. However, this is not an unique solution as there are other solutions using other values for activation slope (Fig. 3 bottom panels). As well, there is no solution in the reduced model that corresponds to the Ca^{2+} channel kinetics used in the template neuromorphic model ($V_{1/2} = -30$ mV, slope = 6 mV). This is evidenced by the lack of white space in the top right panel of Fig. 3 along points where $V_{1/2} = -30$ mV.

4. Discussion and conclusion

Using a reduced two-compartment model we have shown the effects of changes in Ca^{2+} channel kinetics and distribution on the I–V curve. The range of values for the L-type Ca^{2+} channel activation parameters were set according to previously modelled values ($V_{1/2} = -40$ mV, $k = 7$ mV; [2]) and those reported for L-type channels ($V_{1/2} = 0$ mV, $k = 4$ mV; [7]). The lower range of g_c values tested was set according to previously modelled values ($g_c = 0.1$, [2]) and the upper range by the lack of hysteresis in the I–V. The goal of the simulations was to determine if the reduced model could be used to extract additional conclusions on channel kinetics and location from the electrophysiological I–V (see [3]). In its current form, the reduced model was insufficient to uniquely identify the kinetics of the LVA-type Ca^{2+} channels used in the neuromorphic model using the V_{on} and V_{off} of the I–V curve. Similar results were found when HVA-type Ca^{2+} channels were used in the neuromorphic model (results not presented). The large range of g_c values that could be used to match the target I–V curve suggests that the reduced model does not discriminate relative electrotonic distance from the soma.

Two reasons are suggested for this lack of electrotonic discrimination: (1) effect on cell input conductance; and (2) incorrect attenuation. In Fig. 2B the change from $g_c = 0.1$ to 0.5 (mS/cm^2) resulted in an increased input conductance, as evidenced by the increased slope of the I–V curve. This could be corrected by a concomitant decrease in leak conductance, g_{leak}, with an increase in g_c to maintain a constant input conductance. In addition, the current form of the reduced model exhibits direction-dependent voltage attenuation that is opposite to that in the neuromorphic model. In the neuromorphic model there is a greater attenuation of voltage during signal propagation from the dendrites to the soma compared to the reverse direction (see [4]). The failure to account for this behaviour in the reduced model could be corrected by using two g_c's, a smaller one for signal propagation from the dendrite to the soma and a larger one for current moving in the opposite direction. In conclusion, the neuromorphic model remains a better descriptor of the electrophysiological results.

Acknowledgements

We gratefully acknowledge the donation of the morphological data from Dr. R.E. Burke and example XPP source code and guidance from Dr. V. Booth. KEJ acknowledges fellowship support from the Manitoba Neurotrauma Initiative. RMB holds an MHRC Scholar award.

References

[1] R.B. Avery, D. Johnston, Multiple channel types contribute to the low-voltage-activated calcium current in hippocampal CA3 pyramidal neurons, J. Neurosci. 16 (1996) 5567–5582.
[2] V. Booth, J. Rinzel, O. Kiehn, Compartmental model of vertebrate motoneurons for Ca^{2+}-dependent spiking and plateau potentials under pharmacological treatment, J. Neurophysiol. 78 (1997) 3371–3385.
[3] K.P. Carlin, K.E. Jones, Z. Jiang, L.M. Jordan, R.M. Brownstone, Dendritic L-type calcium currents in mouse spinal motoneurones: implications for bistability, Eur. J. Neurosci., in press.
[4] N.T. Carnevale, K.Y. Tsai, B.J. Claiborne, T.H. Brown, The electrotonic transformation: a tool for relating neuronal form to function, in: G. Tesauro, D.S. Touretzky, T.K. Leen (Eds.), Advances in Neural Information Processing Systems, Vol. 7, MIT Press, Cambridge, MA, 1995, pp. 69–76.
[5] S. Cullheim, J.W. Fleshman, L.L. Glenn, R.E. Burke, Membrane area and dendritic structure in type-identified triceps surae alpha-motoneurons, J. Comput. Neurol. 255 (1987) 68–81.
[6] J.W. Fleshman, I. Segev, R.E. Burke, Electrotonic architecture of type-identified alpha-motoneurons in the cat spinal cord. J. Neurophysiol. 60 (1988) 60–85.
[7] A.P. Fox, M.C. Nowycky, R.W. Tsien, Kinetic and pharmacological properties distinguishing three types of calcium current in chick sensory neurones, J. Physiol. (Lond.) 394 (1987) 149–172.
[8] M.L. Hines, N.T. Carnevale, The NEURON simulation environment, Neural Comput. 9 (1997) 1179–1209.